Available online at www.sciencedirect.com
ScienceDirect
Journal of Computational Physics 227 (2008) 5184–5199
JOURNAL OF COMPUTATIONAL PHYSICS
www.elsevier.com/locate/jcp

A hybrid multiscale kinetic Monte Carlo method for simulation of copper electrodeposition ☆

Zheming Zheng [a], Ryan M. Stephens [b], Richard D. Braatz [b], Richard C. Alkire [b], Linda R. Petzold [a,*]

[a] Department of Mechanical Engineering, University of California Santa Barbara, Santa Barbara, CA 93106, USA
[b] Department of Chemical and Biomolecular Engineering, University of Illinois at Urbana-Champaign, Urbana, IL 61801, USA

Received 2 July 2007; received in revised form 20 January 2008; accepted 23 January 2008
Available online 14 February 2008

Abstract

A hybrid multiscale kinetic Monte Carlo (HMKMC) method for speeding up the simulation of copper electrodeposition is presented. The fast diffusion events are simulated deterministically with a heterogeneous diffusion model which considers site-blocking effects of additives. Chemical reactions are simulated by an accelerated (tau-leaping) method for discrete stochastic simulation which adaptively selects exact discrete stochastic simulation for the appropriate reaction whenever that is necessary. The HMKMC method is seen to be accurate and highly efficient.

Keywords: Multiscale simulation; Kinetic Monte Carlo; Stochastic simulation algorithm; Copper electrodeposition

1. Introduction

Electrodeposition processes are used in the fabrication of microelectronic devices and in nanotechnology applications [1–3]. Copper electrodeposition with complex additive systems is used to form interconnections in microelectronic devices [4]. The electrodeposition process involves the diffusion, migration, and convection of solution species in the bulk electrolyte, as well as the reaction and diffusion of surface species at the interface of the solid and the liquid. The surface morphology evolution is controlled via electrolyte additives, some of which are present in very small concentrations, that react with the copper species in solution and on the surface.

In addition to experimental studies [5–8] of the electrodeposition process, computer simulation provides a powerful tool for studying and understanding complex multiscale phenomena. Continuum computational methods [9–12], typically in the form of differential equations, can be used provided that the characteristic

☆ This work was supported by the National Science Foundation under NSF Award NSF/ITR CCF-0428912.
* Corresponding author.
E-mail address: petzold@cs.ucsb.edu (L.R. Petzold).

0021-9991/$ - see front matter © 2008 Elsevier Inc. All rights reserved.
doi:10.1016/j.jcp.2008.01.056

length is significantly greater than the molecular scale, and that the reactant concentrations are large. A stochastic algorithm, the kinetic Monte Carlo (KMC) [13,14] method, has been used to study the molecular features of copper electrodeposition and has been coupled with continuum methods to form a multiscale approach [15–17]. In the KMC approach, the surface reactions and the surface diffusion are modeled as discrete events. However, the time scales of these events may be widely different, resulting in high computational cost.

A number of different approaches have been explored for developing a faster KMC algorithm and a more efficient multiscale approach, including coarse-grained KMC methods [17] and spatially adaptive coarse-grained KMC methods [18,19] which can solve the problem at the mesoscopic scale. Chatterjee et al. [20] proposed a continuum mesoscopic model, which is based on a deterministic partial differential equation (PDE) approximation of the reaction–diffusion system. Multiscale KMC simulations are also available for epitaxial growth applications [21–24].

In the present paper we develop a hybrid multiscale kinetic Monte Carlo (HMKMC) method for efficient simulation of copper electrodeposition in the presence of additives. The challenge of computational efficiency is addressed by partitioning the different reaction channels according to the speed of the reaction and concentration of the reactants. The slower reactions with reactants present in very low concentrations are treated by a detailed stochasatic simulation algorithm (SSA). Reactions with larger reactant concentrations are treated by a non-negativity-preserving tau-leaping SSA method [25–28]. Since diffusion rates on metal surfaces can be very fast with respect to other reaction dynamics, the surface distribution of copper atoms is approximated deterministically by a continuum partial differential equation. The simulation method efficiently solves the surface kinetics of the copper additive chemistry, accurately resolving the surface concentrations of additive complexes, even for species with very small populations.

This paper is organized as follows. We begin in Section 2 with a brief review of the KMC and tau-leaping methods. The detailed HMKMC algorithm is presented in Section 3. In Section 4 we describe our heterogeneous diffusion model for monolayer diffusion of copper. Numerical results are provided in Section 5, and Conclusions are given in Section 6.

2. Background

2.1. The kinetic Monte Carlo method

In this subsection we briefly describe the KMC method and introduce some notation. We use N to denote the number of chemical species in the reaction–diffusion system and M to denote the number of reaction channels. An $N_x \times N_y$ grid is used for the discretization of the interacting surface, where the size of each grid cell is $\Delta L \times \Delta L$.

A pseudo-particle in the simulation is modeled as a cube of size ρ, which is usually much smaller than ΔL. A pseudo-particle corresponds to a site in a grid cell. Different pseudo-particles can be present in the same grid cell, as shown in Fig. 1. A local mean field (local homogeneity) assumption is used inside each grid cell, meaning that the positions of the pseudo-particles in a cell are not tracked; only the number of pseudo-particles in the cell. Let X_{ijk} be the number of pseudo-particles (or population) of species k at grid cell (i,j). In a grid cell, the sum of the numbers of all surface species pseudo-particles is equal to the total number of sites, written as

$$\sum_{k=1}^{N} X_{ijk} = \frac{\Delta L^2}{\rho^2}. \tag{1}$$

Defining a characteristic size ρ_0 and a characteristic population X_0 which satisfy $\Delta L^2 = \rho_0^2 X_0$, Eq. (1) can be rewritten as

$$\sum_{k=1}^{N} \frac{\rho^2}{\rho_0^2} C_{ijk} = 1, \tag{2}$$

where $C_{ijk} = X_{ijk}/X_0$ is the fraction of species k in cell (i,j).

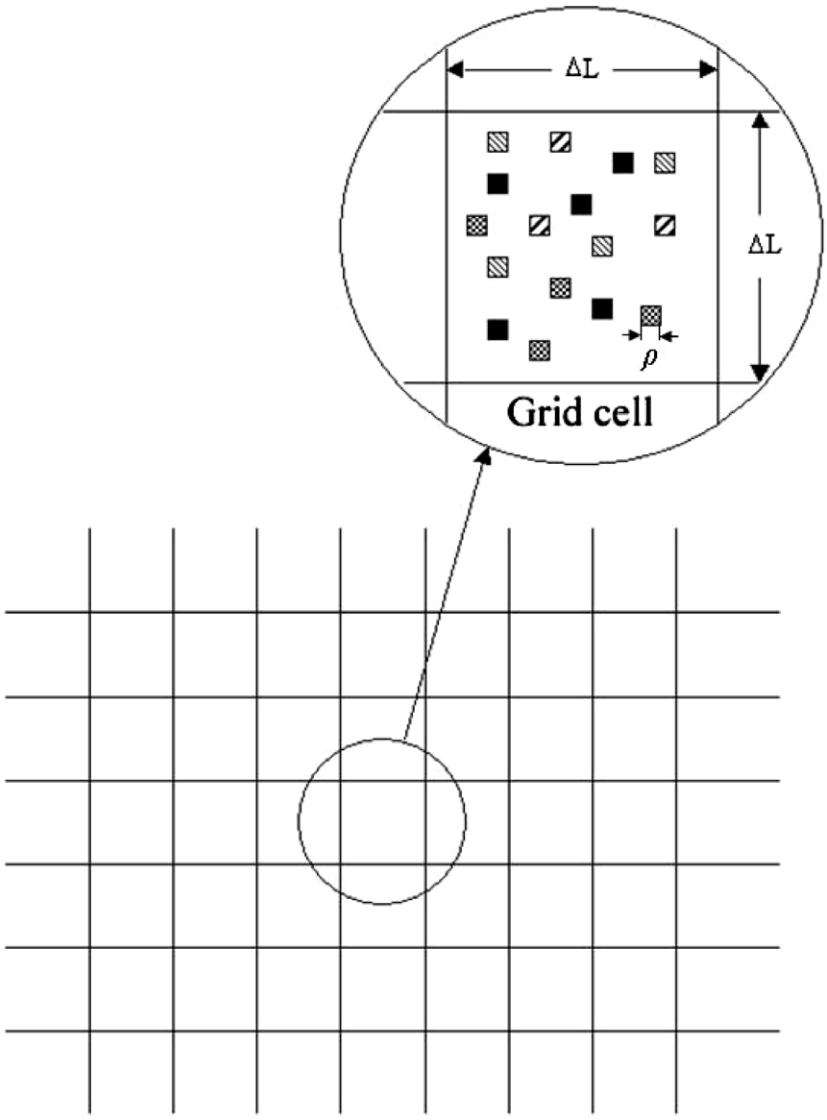

Fig. 1. Grid structure of the HMKMC method. Different pseudo-particles can be present in the same grid cell.

The state vector of the system is denoted by

$$X(t) = \{X(i,j,k) : 1 \leqslant i \leqslant N_x, 1 \leqslant j \leqslant N_y, 1 \leqslant k \leqslant N\},$$

written as

$$X(t) = (X_1(t), \ldots, X_{N_s}(t)),$$

where $N_s = N_x N_y N$. Defined as a reaction in a grid cell, each event is associated with a rate. These event rates

$$\{\text{rate}_{ijk} : 1 \leqslant i \leqslant N_x, 1 \leqslant j \leqslant N_y, 1 \leqslant k \leqslant M\}$$

are also known as the propensity functions $\{a_j, j = 1, \ldots, N_r\}$, with $a_j \,\mathrm{d}t$ giving the probability that event j will occur in the next infinitesimal time interval $[t, t + \mathrm{d}t)$ and $N_r = N_x N_y M$ being the total number of rates. Each event j also has a state change vector $v_j = (v_{1j}, \ldots, v_{N_s j})$, where v_{ij} is the population change in $X_i(t)$ induced by event j. The matrix v is known as the stoichiometric matrix.

The stochastic simulation algorithm (SSA) [29,30] is a KMC-type method which is directed at well-stirred chemically reacting systems. The SSA procedure is defined as follows. Consider a well-stirred, chemically reacting system. Let

$$a_0(x) = \sum_{j=1}^{N_r} a_j(x). \tag{3}$$

The time τ to the next occurring reaction is an exponentially distributed random variable with mean $1/a_0(x)$. The index j of that reaction is an integer random variable with probability $a_j(x)/a_0(x)$. In each step, SSA generates two independent random numbers r_1 and r_2 in $U(0, 1)$ with a uniform distribution on the interval (0, 1). The time for the next reaction to occur is given by $t + \tau$, where τ is given by

$$\tau = \frac{1}{a_0(t)} \log\left(\frac{1}{r_1}\right). \tag{4}$$

The index j for the next reaction is given by the smallest integer satisfying

$$\sum_{l=1}^{j} a_l(t) > r_2 a_0(t). \tag{5}$$

The system states are updated by $X(t + \tau) = X(t) + v_j$. Then the simulation proceeds to the next occurring time, until it reaches the final time.

2.2. Tau-leaping method

The SSA can become very slow if there are fast reactions and/or some chemical species which are present in large populations in the system. The tau-leaping method [25] attempts to accelerate the simulation by asking the question: How many times does each reaction channel fire in the next time interval of length τ? In each step, the tau-leaping method can potentially proceed with many reactions. This is achieved at the cost of some accuracy. Define

$$\begin{aligned} K_j(\tau; x, t) = {} & \text{the number of times, given } X(t) \\ & = x, \text{that reaction } j \text{ will fire in the time interval } [t, t+\tau) \quad (j = 1, \ldots, N_r). \end{aligned} \tag{6}$$

The tau-leaping method assumes the **Leap Condition**: *Require τ to be small enough that the change in the state during $[t, t + \tau)$ will be so small that no propensity function will suffer an appreciable change in its value.* The value of $K_j(\tau; x, t)$ is approximated by the Poisson random variable $P(a_j(x), \tau)$ with mean $a_j(x)\tau$ and variance $a_j(x)\tau$. The basic tau-leaping method is: choose the largest τ that satisfies the Leap Condition. Given $X(t) = x$, generate for each $j = 1, \ldots, N_r$ a sample value of the Poisson random variable $P(a_j(x), \tau)$, and update the state:

$$X^{(et)}(t + \tau) = x + \sum_{j=1}^{N_r} v_j P(a_j(x), \tau), \tag{7}$$

where $P(a_j(x), \tau)$ denotes an independent sample of the Poisson random variable with mean $a_j(x)\tau$. The tau-leaping method tends to the explicit Euler method for the reaction-rate equation as the populations of all chemical species in the system tend to infinity, for fixed τ [25].

To select the τ that satisfies the Leap Condition, Gillespie [25] first proposed a formula based on the Leap Condition. Gillespie and Petzold [26] improved the formula by taking into account the variance, but that formula required the calculation of the Jacobian of the propensity functions $a(x)$, which is expensive and inconvenient. In addition, the above tau-leaping methods can generate negative solutions when the population of some species is very small, since the leaping is based on the Poisson distribution. To resolve this negativity problem, a more rigorous formulation of the tau-leaping method [27] and the corresponding τ-selection strategy [28] were recently proposed by Cao, Gillespie and Petzold. Our work makes use of this strategy in the hybrid multiscale method introduced in Section 3. The τ selection formula is given by (see details in [28])

$$\tau = \min_{i \in I_R} \left\{ \frac{\max\{\epsilon X_i, 1\}}{|\mu_i|}, \frac{\max\{\epsilon X_i, 1\}^2}{\sigma_i^2} \right\}, \tag{8}$$

where

$$\mu_i(x) = \sum_{k=1}^{N_r} v_{ik} a_k(x),$$

$$\sigma_i^2(x) = \sum_{k=1}^{N_r} v_{ik}^2 a_k(x),$$

I_R represents the set of species that are reactants or catalysts of at least one reaction and ϵ is an error control parameter, which is typically around 0.05–0.1, meaning that the population change of each species during a tau-leaping step will not exceed 5–10%.

3. Hybrid multiscale kinetic Monte Carlo method

The proposed simulation algorithm is a hybrid method which draws on ideas from Haseltine and Rawlings [31], Rao and Arkin [32], Cao et al. [33,34] and achieves its efficiency by combining the adaptive non-negativity-preserving tau-leaping SSA method [27,28] with a deterministic (PDE) approximation of the surface diffusion, which is by far the fastest process in the system. The main idea is as follows: to achieve high efficiency in the simulation, reaction channels are partitioned into three regimes. The partitioning of the reactions is done automatically and adaptively.

1. *SSA regime*. This regime includes those reaction channels that are slow and have at least one of its reactants present with a low population (usually less than 20). For reaction channels in this regime, a detailed simulation is necessary because every event in this regime can change the dynamics to a significant extent. The original SSA (see Gillespie [29,30] for details) is applied in this regime.
2. *Poisson regime*. This regime includes those reaction channels such that all the reactants are present with a moderate population (between 20 and 5000). For reaction channels in this regime, one event will not dramatically change the dynamics but stochastic effects should be captured in the simulation. The adaptive non-negativity-preserving tau-leaping SSA method [27,28] is used to simulate the reactions.
3. *Deterministic regime*. In copper electrodeposition problems, surface diffusion is very fast in comparison to surface reactions, and we approximate it deterministically (via a PDE). This can be justified by the slow-scale approximation lemma in [33].

The surface diffusion is modeled by the following PDE:

$$\frac{\partial C}{\partial t} = \nabla \cdot (D \nabla C), \tag{9}$$

where C is the surface concentration of the diffusing species and D is the surface diffusion coefficient. Because of the site-blocking effects of additives on the surface, the surface diffusion is not homogeneous. Instead, it is heterogeneous and dependent on the surface concentration of the additives. A heterogeneous diffusion model is proposed in Section 4 to account for this issue. In our implementation, Eq. (9) is discretized with the finite volume method, yielding

$$\Delta x \Delta y \frac{\mathrm{d}C_{i,j}}{\mathrm{d}t} = J_{i+1,j} - J_{i-1,j} + J_{i,j+1} - J_{i,j-1}, \tag{10}$$

where

$$J_{i+1,j} = D(i+1, j \leftrightarrow i, j) \frac{C_{i+1,j} - C_{i,j}}{\Delta x} \Delta y,$$

$$J_{i-1,j} = D(i-1, j \leftrightarrow i, j) \frac{C_{i,j} - C_{i-1,j}}{\Delta x} \Delta y,$$

$$J_{i,j+1} = D(i,j+1 \leftrightarrow i,j)\frac{C_{i,j+1} - C_{i,j}}{\Delta y}\Delta x,$$
$$J_{i,j-1} = D(i,j-1 \leftrightarrow i,j)\frac{C_{i,j} - C_{i,j-1}}{\Delta y}\Delta x,$$

where $D(i+1,j \leftrightarrow i,j)$ denotes the diffusion coefficient between the cell $(i+1,j)$ and the cell (i,j).

The surface reactions are simulated by the adaptive non-negativity-preserving tau-leaping SSA method [27,28]. In that method, the SSA and Poisson regimes are determined based on whether the corresponding reactants are present in low populations. Those reaction channels with low population reactants are called critical reaction channels and treated by SSA. The remaining reactions are simulated with tau-leaping. Since we treat the fastest process (surface diffusion) deterministically, stiffness is not a big concern in the SSA and Poisson regimes. Thus it is reasonable to use an explicit tau-leaping method.

The algorithm is summarized below:

Algorithm (Hybrid multiscale method):

1. Initialize the system time $t = 0$, set the diffusion time $t_{\text{diff}} = 0$ and the surface diffusion time step-size $= \tau_{\text{diff}}$. The system time t records the real time of the reaction system. The diffusion time is the last time when the surface diffusion is updated and the surface diffusion time step-size determines how often the surface diffusion is updated.
2. Determine the list of critical reactions. In this step, the maximum number of reactions for each channel so that no species will be exhausted is determined by
$$n_j = \min_{v_{ij}<0, 1\leqslant i\leqslant N_s}\left[\frac{x_i}{|v_{ij}|}\right], \tag{11}$$
where the brackets denote "greatest-integer-less-than". A reaction is considered critical if and only if $n_j < N_C$, where N_C is a parameter set to 10.
3. Calculate τ_1 according to the tau-leaping τ selection strategy (8). Let a_0 be the sum of propensity functions of all reaction channels. If the τ-test condition
$$\tau_1 < \frac{\text{MinLeap}}{a_0} \tag{12}$$
is satisfied, go to step 4. Otherwise go to step 5. The parameter MinLeap is currently set to be 10.
4. Since the τ picked up is relatively small, it is more efficient to put all reaction channels into the SSA regime. We use the direct SSA method for all reaction channels. The simulation will repeat the direct SSA method for a certain number of steps before doing another τ-test. This is called a "silence period", which is set to 10 SSA steps. Go to step 6.
5. Calculate the time for the next critical reaction to fire
$$\tau_2 = \frac{\log(1/r)}{\hat{a}_0}, \tag{13}$$
where $\hat{a}_0$ is the sum of the propensities of all critical reaction channels (SSA regime). Denote k_j as the number of firings of reaction j.
   (a) If $\tau_2 \leqslant \tau_1$, take $\tau = \tau_2$. Find J_c as the index of the firing critical reaction. Set $k_{J_c} = 1$ meaning that there is a firing for reaction J_c, and for all other critical reactions set $k_j = 0$. For non-critical Poisson regime reactions, generate k_j as a sample of the Poisson random variable with mean $a_j(x)\tau$.
   (b) If $\tau_2 > \tau_1$, take $\tau = \tau_1$. For all critical reactions set $k_j = 0$. For non-critical Poisson regime reactions, generate k_j as a sample of the Poisson random variable with mean $a_j(x)\tau$.

   Update the system state with the above k's.
6. Update the system time $t \leftarrow t + \tau$.
7. If $t - t_{\text{diff}} > \tau_{\text{diff}}$ then integrate the surface diffusion equation (10) from t_{diff} to $t_{\text{diff}} + \tau_{\text{diff}}$. Update $t_{\text{diff}} \leftarrow t_{\text{diff}} + \tau_{\text{diff}}$. Go to step 2.

In summary, the HMKMC method solves a coupled reaction–diffusion system with a stochastic method for reaction and a deterministic method for diffusion. Specifically, the reactions are simulated by the adaptive non-negativity-preserving tau-leaping SSA method [27,28], and the diffusion equation (10) is first discretized to an ODE by the method-of-lines approach and solved by an adaptive backward Euler method. For simplicity, in this paper we refer to the step-size given by Eq. (4) as the SSA step-size, and the one given by Eq. (8) as the tau-leaping step-size. The HMKMC method adjusts the time step-size adaptively according to the properties of the system.

4. Heterogeneous surface diffusion modeling

As discussed above, the site-blocking effects of additives on the surface require a heterogeneous treatment of surface diffusion. In this section we derive the relationship between the heterogeneous diffusion coefficient and the surface concentration of the diffusing species and the additives.

We define two grid cells k and l on the discretized space, for the two scenarios shown in Figs. 2 and 3. In the first simplified scenario, i.e., Fig. 2, the pseudo-particle in grid cell k can diffuse to any position in cell l, as well as three other surface positions (north, west, and south), and the diffusion is treated homogeneously, in that the diffusion coefficients in the four directions are assumed to be the same. Let C_k and C_l denote the concentrations in grid cells k and l, respectively. The rates of the diffusion events are written as

$$r(k \to l) = \frac{\Gamma}{4a} C_k a^2, \tag{14}$$

$$r(l \to k) = \frac{\Gamma}{4a} C_l a^2, \tag{15}$$

where Γ is the jump frequency (number of jump attempts per pseudo-particle per second) and a is the grid size. In the above equations, Γ is divided by 4 for the 4 jump directions in 2D diffusion, the number of diffusing pseudo-particles in cell k is $C_k a^2$, and Eq. (14) is the number of pseudo-particles that cross the interface (a line of length a) between cells k and l from k to l per unit length per unit time (s).

Thus the net flux J_d from k to l is

$$J_d = r(k \to l) - r(l \to k) = \frac{\Gamma a}{4}(C_k - C_l), \tag{16}$$

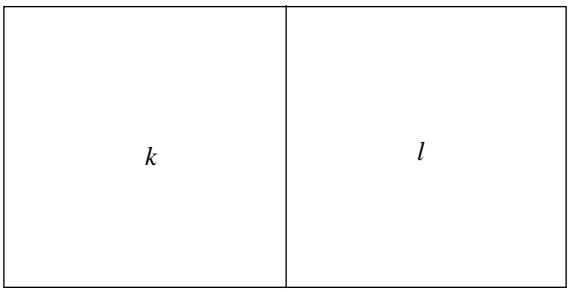

Fig. 2. Discrete diffusion scenario 1 in monolayer diffusion.

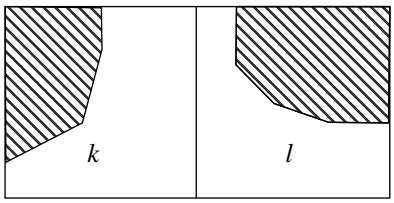

Fig. 3. Discrete diffusion scenario 2 in monolayer diffusion.

which should match the flux based on the continuous equation,

$$J_c = D(k \leftrightarrow l)\frac{C_k - C_l}{a}. \tag{17}$$

Thus

$$\frac{\Gamma a}{4}(C_k - C_l) = D(k \leftrightarrow l)\frac{C_k - C_l}{a}, \tag{18}$$

which yields $D(k \leftrightarrow l) = \frac{1}{4}\Gamma a^2$.

In the second more general scenario in Fig. 3, the diffusing pseudo-particle can only diffuse from the shaded area (occupied sites) to the blank area (vacant sites). The rates of diffusion events are not only proportional to the number of available diffusing pseudo-particles in the initial cell, but also proportional to the number of available vacant sites in the final cell. These take the following form [35]:

$$r(k \to l) = \frac{\Gamma}{4a}C_k a^2(1 - f_l), \tag{19}$$

$$r(l \to k) = \frac{\Gamma}{4a}C_l a^2(1 - f_k), \tag{20}$$

where Γ is the jump frequency, a is the grid size, f_k and f_l are the fractions of occupied sites in cells k and l respectively, and f_k is equal to the total number of occupied sites divided by the total number of sites in grid cell k, written as

$$f_k = \frac{(C_k + D_k + E_k + \cdots)a^2}{a^2/\rho^2} = A_k\rho^2, \tag{21}$$

where ρ is the size of a pseudo-particle (or a site), $A_k = (C_k + D_k + E_k + \cdots)$ is the concentration of occupied sites in cell k, and C, D, E, ... are the concentrations of different surface species.

The net flux J_d from k to l is given by

$$J_d = r(k \to l) - r(l \to k) = \frac{\Gamma a}{4}[C_k - C_l - (C_k A_l - C_l A_k)\rho^2], \tag{22}$$

which should match the flux from the continuous diffusion equation

$$J_c = D(k \leftrightarrow l)\frac{C_k - C_l}{a}. \tag{23}$$

Thus

$$D(k \leftrightarrow l) = \frac{1}{4}\Gamma a^2\frac{C_k - C_l - (C_k A_l - C_l A_k)\rho^2}{C_k - C_l}. \tag{24}$$

Thus the diffusion coefficients associated with pseudo-particles are generally heterogeneous and concentration-dependent. In the special case where there is only one surface species, i.e., the diffusing species is the only surface species on the surface, we have $C_k = A_k$. Then Eq. (24) reduces to $D(k \leftrightarrow l) = \frac{1}{4}\Gamma a^2$, the homogeneous diffusion case. In the special case where two surface species are present on the surface (a diffusing non-blocking copper species with concentration C_k and a non-diffusing blocking additive with concentration D_k) and the concentration of the additive is uniform on the surface, with fraction given by

$$\theta = \frac{D_k a^2}{a^2/\rho^2} = \rho^2 D_k, \tag{25}$$

the diffusion coefficient is

$$D(k \leftrightarrow l) = \frac{1}{4}\Gamma a^2(1 - \theta). \tag{26}$$

The presence of the additive (meaning a positive θ) results in a smaller effective diffusion coefficient.

5. Numerical simulations

5.1. Adsorption–desorption kinetics

The HMKMC method is first applied to the following reversible adsorption–desorption reactions:

$$A_{\mathrm{aq}} \Longleftrightarrow [k_{\mathrm{a}}]k_{\mathrm{d}}B_{\mathrm{ads}}, \tag{27}$$

where A_{aq} indicates that A is an aqueous solution species, B_{ads} indicates that B is an adsorbed surface species, and k_{a} and k_{d} are the forward adsorption rate constant and backward desorption rate constant, respectively. In this test problem, diffusion is not considered and the reactions are treated by the adaptive non-negativity-preserving tau-leaping SSA method in the HMKMC method. For this simple problem, an ODE can be derived which directly models the evolution of the surface-averaged coverage of B and solved analytically. The ODE describing the evolution of the surface coverage of B, denoted by θ, is

$$\frac{\mathrm{d}\theta}{\mathrm{d}t} = k_{\mathrm{a}}C_A(1-\theta) - k_{\mathrm{d}}\theta, \tag{28}$$

where C_A is the concentration of A asymptotically close to the surface. With initial condition $\theta(t=0)=0$, the analytical solution for Eq. (28) is

$$\theta(t) = \frac{k_{\mathrm{a}}C_A}{k_{\mathrm{a}}C_A + k_{\mathrm{d}}}(1 - \mathrm{e}^{-(k_{\mathrm{a}}C_A+k_{\mathrm{d}})t}). \tag{29}$$

At equilibrium, $\frac{\mathrm{d}\theta}{\mathrm{d}t}=0$ and $\theta = \frac{k_{\mathrm{a}}C_A}{k_{\mathrm{a}}C_A+k_{\mathrm{d}}}$.

The following simulation results use the parameters $C_A = 30\ \ \mathrm{mol/m^3}$, $k_{\mathrm{a}} = 0.4\ \mathrm{m^3/(mol\ s)}$ and $k_{\mathrm{d}} = 151/\mathrm{s}$. The equilibrium surface coverage is $\theta = \frac{k_{\mathrm{a}}C_A}{k_{\mathrm{a}}C_A+k_{\mathrm{d}}} = 0.44$. For the HMKMC method, a 100×100 grid with grid length $\Delta L = 5 \times 10^{-8}$ m was used.

For this problem, it is not possible to do an atomic-scale regular KMC simulation. The length scales of key features on the surface are much larger than the scale of an atom. A typical atomic force microscopy image that is large enough to include several nuclei on a surface are 5 μm on a side, which consists of $(5 \times 10^{-6})/(1.28 \times 10^{-10}) =\sim 40,000$ lattice points on side. Regular KMC simulation is too computationally expensive to be carried out for a problem with more than 1 billion ($\sim 40,000^2$) lattice points.

As an assessment of accuracy, Fig. 4 compares the results of HMKMC simulation with the coverage (29) which would be obtained by using a sufficiently large number of lattice points or as the average of a large number of KMC simulation runs. Shown in Table 1, the computation is faster for the largest X_0 (implying less coarse-graining), in which case reactions are more likely to be modeled in the Poisson regime, and the advantages of tau-leaping are fully utilized. This value of $X_0 = 1.5 \times 10^5$ is the largest possible number for the given ΔL, as $\rho = 1.28 \times 10^{-10}$ m is the physical size of an atom (the size of a pseudo-particle cannot be smaller than that of an atom). With decreasing X_0 (see Fig. 4(A)–(C)), the time step-size chosen by the HMKMC method gradually reduces from the larger tau-leaping step-size to the smaller SSA step-size, resulting in an increase in CPU time. The accuracy of the HMKMC method shown in Fig. 4(A)–(C) is good, with Fig. 4(C) having the best accuracy since it uses the smallest time step-size; however, it requires the largest CPU time.

For $X_0 = 1$, or equivalently, $\rho = \Delta L$, the pseudo-particle is the same size as a grid cell, which has been used in the regular coarse-grained KMC methods (e.g., [17]). The HMKMC method for $X_0 > 1$ (Fig. 4(A)–(C)) is nearly as accurate as the regular coarse-grained KMC method ($X_0 = 1$, Fig. 4(D)), with less stochastic fluctuations. An atomic-scale KMC simulation, if it could be carried out, would show negligible stochastic fluctuations in the coverage for the surface area of these simulations – indicating that the fluctuations in the regular coarse-grained KMC method are not physical. Cases C and D use the SSA step-size selection algorithm, but because there are fewer particles in Case D, it uses a larger time step-size than Case C. Case D takes less computation time than Case C but its solution is not as accurate and meanders above and below the exact analytical solution.

In summary, compared to the regular coarse-grained KMC method, the HMKMC method (with large X_0 numbers) is efficient while preserving reasonably good accuracy.

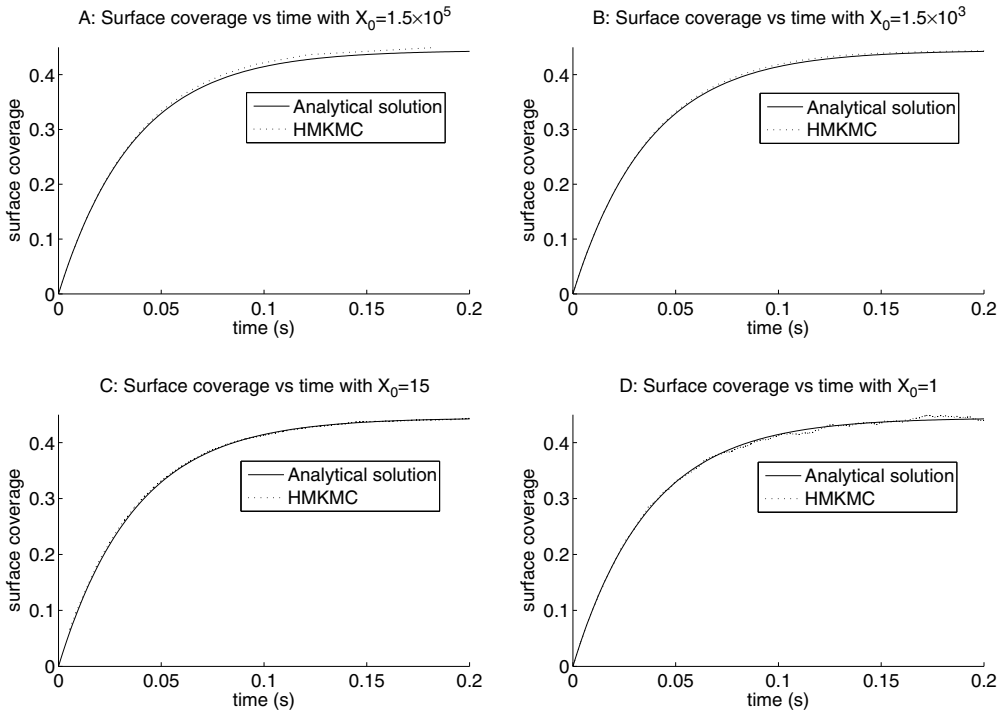

Fig. 4. Surface coverage comparison between the HMKMC solutions and the analytical solution for (A) $X_0 = 1.5 \times 10^5$; (B) $X_0 = 1.5 \times 10^3$; (C) $X_0 = 15$; (D) $X_0 = 1$.

Table 1
Parameters and CPU times in the adsorption–desorption kinetics test

Fig. 4	ρ (m)	$X_0 = \Delta L^2/\rho^2$	CPU time (s)
A	1.28×10^{-10}	1.5×10^5	16.15
B	1.28×10^{-9}	1.5×10^3	37.55
C	1.28×10^{-8}	15	2150.3
D	5×10^{-8}	1	150.65

5.2. Copper electrodeposition kinetics

In this test the HMKMC method was applied to copper electrodeposition, without surface diffusion and bulk solution diffusion, and was compared to the solution of the ODE rate equation [36,37]. The copper electrodeposition mechanism [36,37] and the coefficients used are shown in Table 2.

The HMKMC method used a 64×64 grid, grid length $\Delta L = 5 \times 10^{-8}$ m, and pseudo-particle size $\rho = 1.28 \times 10^{-10}$ m. The numerical solution is computed to the time $T = 0.5$ s. The spatially-averaged concentrations of the surface species are plotted in Fig. 5, in which CuCl denotes the cuprous chloride, CuClPEG denotes Cu(I)-Cl-PEG, PEG denotes polyethylene glycol, CuTh denotes Cu(I)-thiolate, CuHIT denotes Cu(I)-HIT and HIT denotes 1-(2-hydroxyethyl)-2-imidazolidinethione. The ODE solution coincides with the HMKMC solution. Fig. 6 focuses in on the concentration of Cu(I)-HIT, which is the species with lowest concentration, for HMKMC solutions with $X_0 = 1.5 \times 10^5$ and $X_0 = 1.5 \times 10^3$, together with the ODE solution. The agreement of the numerical solution with the ODE solution becomes worse with decreasing X_0. Moreover, the computation time (8403 s) of the case $X_0 = 1.5 \times 10^3$ is greater than that of the case $X_0 = 1.5 \times 10^5$ (5605 s). If we further decrease X_0, the computation becomes even slower and the numerical solution rougher (as one might expect due to small-population effects).

Table 2
Surface reactions in copper electrodeposition mechanism

No.	Reactions	k	α	E^0 (V)
1	$Cu^{2+}_{aq} + e^- \rightarrow Cu^+_{aq}$	0.111	0.5	−0.5
2	$Cu^+_{aq} + e^- \rightarrow Cu_s$	0.0129	0.5	−0.12
3	$Cu_s \rightarrow Cu^+_{aq} + e^-$	0.01	0.5	−0.12
4	$Cu^+_{aq} + Cl^-_{aq} \rightarrow CuCl_{ads}$	5.0		
5	$CuCl_{ads} \rightarrow Cu^+_{aq} + Cl^-_{aq}$	10.0		
6	$CuCl_{ads} + e^- \rightarrow Cu_s + Cl^-_{aq}$	0.01	0.5	−0.12
7	$CuCl_{ads} + PEG_{aq} \rightarrow CuClPEG_{ads}$	110.3		
8	$CuClPEG_{ads} \rightarrow CuCl_{ads} + PEG_{aq}$	1.0		
9	$SPS_{aq} + 2e^- \rightarrow 2thiolate^-$	1.0e−3	0.5	−0.4
10	$Cu^+_{aq} + MPS_{aq} \rightarrow Cu(I)thiolate_{ads} + H^+_{aq}$	10.0		
11	$Cu(I)thiolate_{ads} + H^+_{aq} \rightarrow Cu^+_{aq} + MPS_{aq}$	1.0e−5		
12	$Cu^+_{aq} + Cu(I)thiolate_{ads} + e^- \rightarrow Cu(I)thiolate_{ads} + Cu_s$	0.0211	0.5	−0.12
13	$Cu(I)thiolate_{ads} + HIT_{aq} \rightarrow Cu(I)HIT_{ads} + MPS_{aq}$	20.0		
14	$Cu(I)HIT_{ads} + H^+_{aq} + e^- \rightarrow HIT_{aq} + Cu_s$	2.0e−7	0.5	−0.12

k is the reaction rate constant, α is the charge transfer coefficient and E^0 is the rest potential.

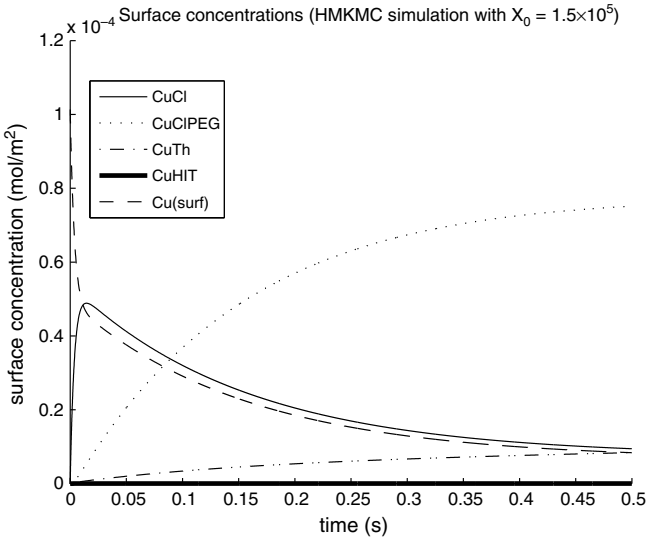

Fig. 5. Concentrations of surface species vs. time. [*Note*: the concentration of CuHIT is small compared to others and almost coincides with the x-axis.]

These observations agree with those in Section 5.1, i.e., the HMKMC method is efficient and accurate with a large X_0. A snapshot of the deposited surface by the computer simulation is given in Fig. 7, where the grey level shows the density of deposited copper.

5.3. Surface diffusion

This section describes the determination of the diffusion time step-size for coupling of reaction and diffusion and verification of the surface diffusion model of the HMKMC method.

5.3.1. Diffusion time step-size determination

This test considers the coupled reaction–diffusion system in which the adsorption–desorption reactions (27) are allowed only in the center grid cell of a 100×100 grid and the surface diffusion of B pseudo-particles occurs on the whole 100×100 grid. This corresponds to the physical situation in which an open copper site

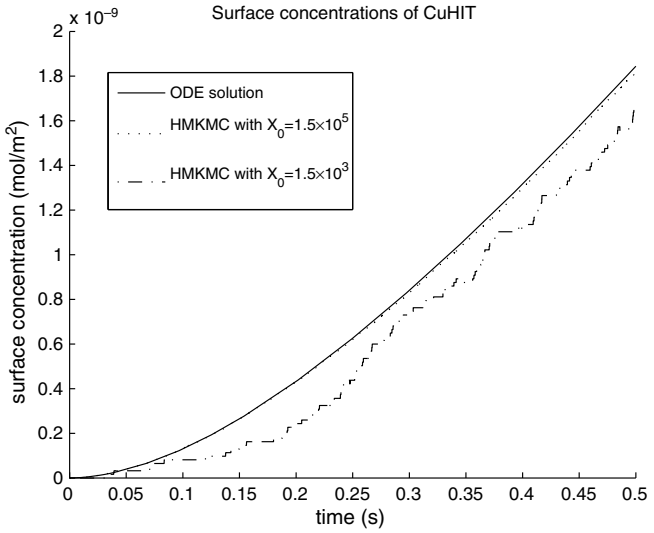

Fig. 6. Comparison of Cu(I)-HIT concentrations.

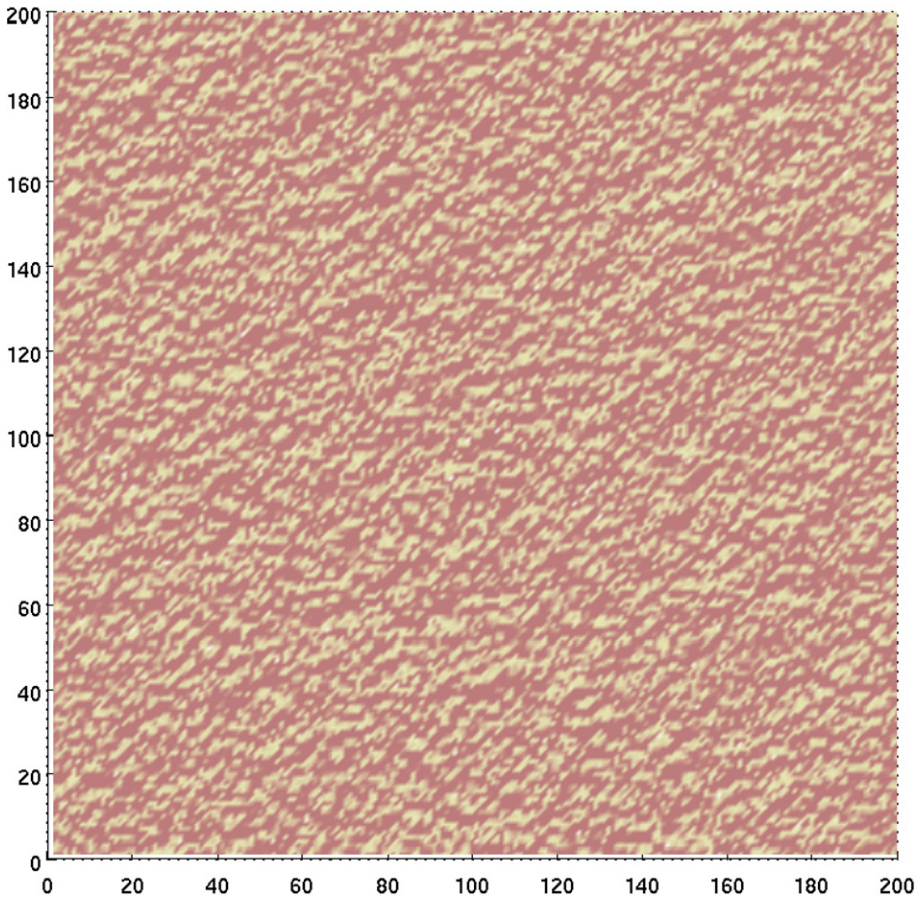

Fig. 7. A plot of the deposited surface.

is surrounded by molecules (e.g., PEG) that block electrodeposition but allow surface diffusion to occur under the molecules.

The PDE for this system is

$$\frac{\partial C_{i,j}}{\partial t} = D\nabla^2 C_{i,j} + f_{i,j}, \tag{30}$$

where

$$f_{i,j} = \begin{cases} k_a C_A(1 - C_{i,j}) - k_d C_{i,j} & (i,j) \text{ is the center grid cell,} \\ 0 & \text{otherwise,} \end{cases} \tag{31}$$

and $C_{i,j}$ is the fractional coverage of B. The parameters were set as $C_A = 30\ \text{mol/m}^3$, $k_a = 0.004\ \text{m}^3/(\text{mol s})$, $k_d = 0.151/\text{s}$, and $D = 1.0 \times 10^{-12}\ \text{m}^2/\text{s}$. The solution was computed to the time $T = 0.2$ s.

The maximal concentration in the center grid cell obtained by directly solving the PDE (30) is $C_{\max} = 2.0091 \times 10^{-4}$. For the HMKMC method with a 100×100 grid, $\Delta L = 5 \times 10^{-8}$ m, $X_0 = 1.5 \times 10^5$ ($\rho = 1.28 \times 10^{-9}$ m), the diffusion time step-size was varied from 1.0×10^{-2} to 1.0×10^{-6}, to assess the convergence. The comparison of maximal concentrations for varying diffusion time step-sizes in Fig. 8 indicates that the HMKMC solution is convergent with decreasing diffusion time step-sizes. In the HMKMC method, the remaining numerical simulations use a predetermined diffusion time step-size of $\tau_{\text{diff}} = 1.0 \times 10^{-5}$ s, which is small enough to maintain accuracy.

5.3.2. Surface diffusion verification

In this numerical experiment we test the diffusion model in Section 4. The HMKMC algorithm is compared to a standard KMC model [38] described in the Appendix, for the case of copper diffusion on a surface partially occupied by a simple blocking additive complex. The copper diffuses freely on the underlying metal surface and on deposited copper, but it does not diffuse onto the sites occupied by additive species. For this comparison, there is no deposition or dissolution of metal, nor are there any additional reaction kinetics. The diffusing species are all present on the surface at the beginning of the simulation. The problem domain is a 1 μ m × 1 μm square, which is discretized to a 100×100 grid with grid length $\Delta L = 1.0 \times 10^{-8}$ m. This test uses a spatially uniform additive coverage $\theta = 0.05$. The initial concentration was set to 0 in one half of the plane and $0.1(1 - \theta)$ in the other half of the plane. As shown in Eq. (26), the effective diffusion coefficient is $D_e = \frac{1}{4}\Gamma a^2(1 - \theta) = D(1 - \theta)$. An analytical solution for this problem is obtained in [39]

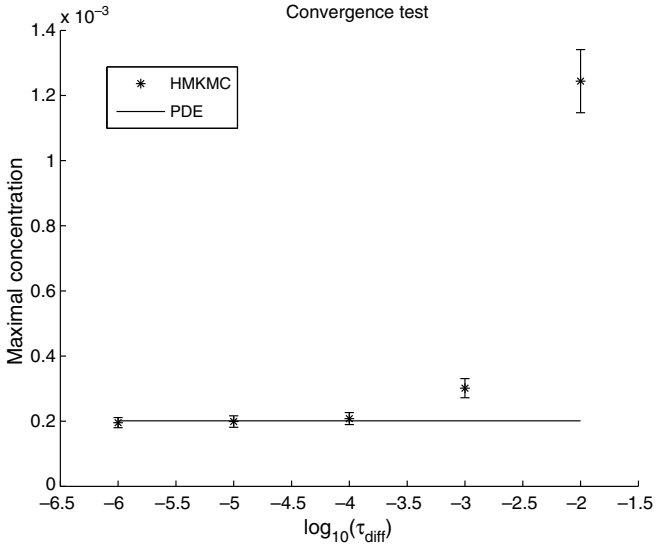

Fig. 8. Convergence test for the coupling of reaction and diffusion.

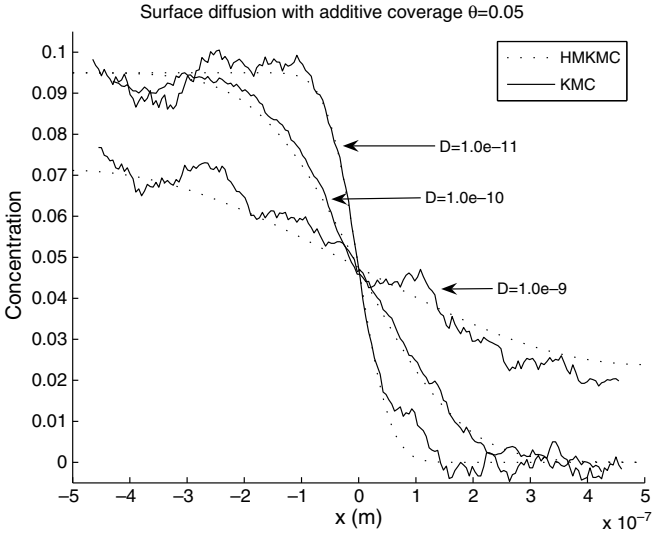

Fig. 9. Concentration profile after 1 s of diffusion.

$$C(x,t) = \frac{1}{2} C_0 \operatorname{erfc} \frac{x}{\left(2\sqrt{(D_e t)}\right)}, \tag{32}$$

where $C_0 = 0.1(1-\theta)$ and erfc is the complementary error function. Fig. 9 plots the concentration profile after 1 s of diffusion for different diffusion coefficients. The deterministic HMKMC solutions completely overlap with the analytical solution, and agree well with the previous stochastic KMC solutions.

6. Conclusions

In this paper a hybrid multiscale kinetic Monte Carlo (HMKMC) method has been introduced to accelerate the simulation of copper electrodeposition. The reactions are simulated by an adaptive non-negativity-preserving tau-leaping stochastic simulation algorithm (SSA), where an appropriate step-size is selected adaptively by the algorithm for best speed-up while retaining a desired accuracy. The fast diffusion events are solved deterministically with a heterogeneous diffusion model which considers site-blocking effects of additives.

Compared to fully deterministic methods (ODEs and PDEs), this stochastic-deterministic hybrid KMC method retains the stochastic fluctuations which are important in accurately capturing all of the small-scale dynamics. On the other hand, by treating the surface diffusion deterministically, the capability to simulate larger problems is significantly improved. As demonstrated by the numerical examples, the simulation is significantly accelerated from the coarse-grained KMC methods and maintains good accuracy. A heterogeneous diffusion model has been proposed for monolayer diffusion of copper, which has been verified by numerical experiments.

Acknowledgments

We thank Mohan Karulkar for the ODE model of the copper electrodeposition mechanism.

Appendix

The KMC algorithm employed here is similar to that described by Levi and Kotrla [40] and Battaile et al. [41] used for simulations of crystal growth. Details are available in Ref. [38].

1. Choose a random number, U_1, from a uniform distribution in the range $(0,1)$.
2. Select the transition event from the list by selecting the first index s for which $\sum_{j=1}^{s} n_j r_j \geqslant U_1$.

3. Choose the lattice site from n_s randomly by generating another random number U_2, uniformly distributed in $(0,1)$.
4. Implement the transition event s at the chosen site with rate r_s.
5. Update all r_j that changed as a result of Step 3.
6. Advance the time in the simulations with time step-size $\tau = \frac{1}{\sum_j n_j r_j}$. Return to Step 1.

In more detail, the rates are binned by type in order to speed up the simulations. The computational expense is reduced by using structured lists when coding the KMC algorithm:

1. Information about each rate is stored in a matrix. The site number is unique for each site on the surface. Periodic boundary conditions are used in the x and y directions.
2. At the beginning of the simulation, the rates for all possible moves are tabulated and cataloged. These rates are only recalculated when a move occurs at a site or one of its eight nearest neighbors.
3. All of the possible rates in the system are binned to create a list that is used to select which events occur.
4. The rates are normalized and a uniformly distributed random number U_1 is generated on the interval $(0,1)$.
5. Once the random number is generated, the appropriate event is selected from the list.
6. An instance of that event is selected randomly from the bin for that rate by generating another uniformly distributed random number U_2 in $(0,1)$ and the action is executed.
7. The appropriate neighbor rates are updated in the site list depending on the action that is taken.
8. The time in the system is updated and the process is repeated.

This (2+1)D KMC model uses the rate-based approach which formulates all actions in terms of rates and checks a single site per Monte Carlo time step. Null events are eliminated in this approach. There is a single Monte Carlo time step in the simulation that is a function of the species and their associated rates. It is possible to simulate the effect of low concentration additives and steric effects with this KMC formulation.

References

[1] R.C. Alkire, R.D. Braatz, Electrochemical engineering in an age of discovery and innovation, AIChe J. 50 (9) (2004) 2000.
[2] V. Srinivasan, L. Lipp, Report of the electrolytic industries for the year 2002, J. Electrochem. Soc. 150 (2003) K15.
[3] National Materials Advisory Board. New horizons in electrochemical science and technology, Technical Report, National Academy Press, Washington, DC, 1986.
[4] T.O. Drews, S. Krishnan, J.C. Alameda, D. Gannon, R.D. Braatz, R.C. Alkire, Multiscale simulation of copper electrodeposition onto a resistive substrate, IBM J. Res. Dev. 49 (1) (2005).
[5] J. Horkans Jr., C. Cabral, K.P. Rodbell, C. Parks, M.A. Gribelyuk, S. Malhotra, P.C. Andricacos, Trends in properties of electroplated Cu with plating conditions and chemistry, in: ECS Proceedings Volume: Electrochemical Processing in ULSI Fabrication III, 2000.
[6] T.P. Moffat, J.E. Bonevich, W.H. Huber, A. Stanishevsky, D.R. Kelly, G.R. Stafford, D. Josell, Superconformal electrodeposition of copper in 500–90 nm features, J. Electrochem. Soc. 147 (2000) 4524.
[7] D.M. Kolb, The initial stages of metal deposition as viewed by scanning tunneling microscopy, Adv. Electrochem. Sci. Eng. 7 (2002).
[8] E. Budevski, G. Staikov, W.J. Lorenz, Electrocrystallization nucleation and growth phenomena, Electrochim. Acta 45 (2000) 2559.
[9] T.P. Moffat, D. Wheeler, W.H. Huber, D. Josell, Superconformal electrodeposition of copper, Electrochem. Solid State Lett. 4 (2001) C26.
[10] T.P. Merchant, M.K. Gobbert, T.S. Cale, L.J. Borucki, Multiple scale integrated modeling of deposition processes, Thin Solid Films 365 (2000) 368.
[11] M. Georgiadou, D. Veyret, R.L. Sani, R.C. Alkire, Simulation of shape evolution during electrodeposition of copper in the presence of additive, J. Electrochem. Soc. 148 (2001) C54.
[12] W.N. Gill, D.J. Duquette, D. Varadarajan, Mass transfer models for the electrodeposition of copper with a buffering agent, J. Electrochem. Soc. 148 (2001) C289.
[13] A.B. Bortz, M.H. Kalos, J.L. Lebowitz, A new algorithm for Monte Carlo simulation of Ising spin systems, J. Comput. Phys. 17 (1975) 10.
[14] K.A. Fichthorn, W.H. Weinberg, Theoretical foundations of dynamical Monte Carlo simulations, J. Chem. Phys. 95 (2) (1991) 1090.
[15] T.O. Drews, A. Radisic, J. Erlebacher, R.D. Braatz, P.C. Searson, R.C. Alkire, Stochastic simulation of the early stages of kinetically limited electrodeposition, J. Electrochem. Soc. 153 (2006) C434.
[16] T.O. Drews, E.G. Webb, D.L. Ma, J. Alameda, R.D. Braatz, R.C. Alkire, Coupled mesoscale-continuum simulations of copper electrodeposition in a trench, AIChe J. 50 (1) (2004) 226.

[17] T.O. Drews, R.D. Braatz, R.C. Alkire, Coarse-grained kinetic Monte Carlo simulation of copper electrodeposition with additives, Int. J. Multiscale Comput. Eng. 2 (2) (2004) 313.
[18] M.A. Katsoulakis, D.G. Vlachos, Coarse-grained stochastic processes and kinetic Monte Carlo simulations for the diffusion of interacting particles, J. Chem. Phys. 119 (2003) 9412.
[19] M.A. Katsoulakis, A.J. Majda, D.G. Vlachos, Coarse-grained stochastic processes and Monte Carlo simulations in lattice systems, J. Comput. Phys. 186 (2003) 250.
[20] A. Chatterjee, M.A. Snyder, D.G. Vlachos, Mesoscopic modeling of chemical reactivity, Chem. Eng. Sci. 59 (2004) 5559.
[21] T.P. Schulze, P. Smereka, E. Weinan, Coupling kinetic Monte-Carlo and continuum models with application to epitaxial growth, J. Comput. Phys. 189 (2003) 197.
[22] C.C. Chou, M.L. Falk, Multiscale diffusion Monte Carlo simulation of epitaxial growth, J. Comput. Phys. 217 (2006) 519.
[23] L. Mandreoli, J. Neugebauer, R. Kunert, E. Schöll, Adatom density kinetic Monte Carlo: a hybrid approach to perform epitaxial growth simulations, Phys. Rev. B 68 (2003) 155429.
[24] J.P. DeVita, L.M. Sander, P. Smereka, Multiscale kinetic Monte Carlo algorithm for simulating epitaxial growth, Phys. Rev. B 72 (2005) 205421.
[25] D. Gillespie, Approximate accelerated stochastic simulation of chemically reacting systems, J. Chem. Phys. 115 (2001) 1716.
[26] D. Gillespie, L. Petzold, Improved leap-size selection for accelerated stochastic simulation, J. Chem. Phys. 119 (2003) 8229–8234.
[27] Y. Cao, D. Gillespie, L. Petzold, Avoiding negative populations in explicit Poisson tau-leaping, J. Chem. Phys. 123 (2005) 054104.
[28] Y. Cao, D. Gillespie, L. Petzold, Efficient stepsize selection for the tau-leaping method, J. Chem. Phys. 124 (2006) 044109.
[29] D. Gillespie, A general method for numerically simulating the stochastic time evolution of coupled chemical reactions, J. Comput. Phys. 22 (1976) 403–434.
[30] D. Gillespie, Exact stochastic simulation of coupled chemical reactions, J. Phys. Chem. 81 (1977) 2340–2361.
[31] E. Haseltine, J. Rawlings, Approximate simulation of coupled fast and slow reactions for stochastic chemical kinetics, J. Chem. Phys. 117 (2002) 6959–6969.
[32] C. Rao, A. Arkin, Stochastic chemical kinetics and the quasi steady-state assumption: application to the Gillespie algorithm, J. Chem. Phys. 118 (2003) 4999–5010.
[33] Y. Cao, D. Gillespie, L. Petzold, The slow-scale stochastic simulation algorithm, J. Chem. Phys. 122 (2005) 014116.
[34] Y. Cao, D. Gillespie, L. Petzold, Multiscale stochastic simulation algorithm with stochastic partial equilibrium assumption for chemically reacting systems, J. Comput. Phys. 206 (2005) 395–411.
[35] A. Chatterjee, D.G. Vlachos, M.A. Katsoulakis, Spatially adaptive lattice coarse-grained Monte Carlo simulations for diffusion of interacting molecules, J. Chem. Phys. 121 (22) (2004) 11420.
[36] F. Xue, Investigation of the Influence of a Model Additive System on Copper Electrodeposition: Integration of Experiments on the Surface Morphology Evolution with Multiscale Simulation, PhD Thesis, University of Illinois at Urbana-Champaign, 2005.
[37] X. Li, T.O. Drews, E. Rusli, F. Xue, Y. He, R. Braatz, R. Alkire, Effect of additives on shape evolution during electrodeposition I. Multiscale simulation with dynamically coupled kinetic Monte Carlo and moving-boundary finite-volume codes, J. Electrochem. Soc. 154 (2007) D230.
[38] T.O. Drews, Multiscale Simulations of Nanofabricated Structures: Application to Copper Electrodeposition for Electronic Devices, PhD Thesis, University of Illinois at Urbana-Champaign, 2004.
[39] J. Crank, The Mathematics of Diffusion, Oxford University Press, 1975.
[40] A.C. Levi, M.J. Kotrla, Review article: Theory and simulation of crystal growth, Phys. Condens. Matter 9 (1997) 299.
[41] C.C. Battaile, D.J. Srolovitz, J.E. Butler, A kinetic Monte Carlo method for the atomic-scale simulation of chemical vapor deposition: application to diamond, J. Appl. Phys. 82 (1997) 6293.